Journal of Mechanisms and Robotics. Received March 09, 2015;
Accepted manuscript posted July 10, 2015. doi:10.1115/1.4031026

A Design System for Eight-bar Linkages as Constrained 4R Serial Chains

Kaustubh H. Sonawale
Graduate Student Researcher
Email: ksonawal@uci.edu

J. Michael McCarthy
Professor, Fellow of ASME
Email: jmmccart@uci.edu

Robotics and Automation Laboratory
Department of Mechanical and Aerospace Engineering
University of California, Irvine
Irvine, CA 92697

This paper presents a design system for planar eight-bar linkages that adds three RR constraints to a user specified 4R serial chain. There are 100 *ways in which these constraints can be added to yield as many as* 3951 *different linkages. An analysis routine based on the Dixon determinant evaluates the performance of each linkage candidate and determines the feasible designs that reach the task positions in a single assembly. A random search within the user specified tolerance zones around the task specifications is iterated in order to increase the number of linkage candidates and feasible designs. The methodology is demonstrated with the design of rectilinear eight-bar linkages that guide an end-effector through five parallel positions along a straight line.*

1 Introduction

This paper presents a design system for eight-bar linkages that begins with a 4R serial chain shown in Figure 1 and adds three RR constraints to obtain a one degree-of-freedom linkage. This approach was introduced by Soh et al. [1, 2], who added two RR chains to a planar 3R serial chain to design six-bar linkages.

The design system includes a systematic procedure that yields 100 ways to attach three RR constraints to a 4R chain to obtain an eight-bar linkage, and can generate as many as 3951 candidate designs in one iteration. The adjacency matrix of the resulting linkage is used to formulate and analyze each candidate to identify feasible eight-bar linkage designs. The system iterates this process for random variations of the required task within tolerance zones provided by the designer in order to generate a large number of successful designs.

The design procedure is demonstrated with a task to find linkages that guide a task frame through five parallel positions on a straight line in order to design rectilinear eight-bar linkages.

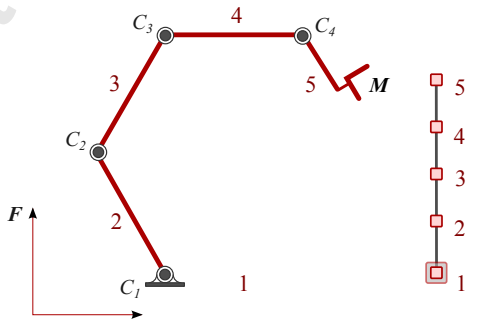

Fig. 1. A 4R serial chain robot together with its linkage graph. Link 1 is the ground link and link 5 is the end-effector link.

2 Literature Review

Central to this design system is the calculation of an RR constraint that connects two bodies in relative movement. This is a generalization of Burmester's [3] formulation of the synthesis or RR cranks to design a four-bar linkage [4, 5].

The designer specifies five task positions for the end-effector of a planar 4R serial chain. The inverse kinematics of this redundant manipulator is used to define the relative positions of every link in each of these task positions, [6, 7]. The synthesis routine follows the procedure outlined by Soh et al. [1], which is also described in McCarthy and Soh [8].

This design system uses the adjacency matrix of the eight-bar linkage graph to manage the sequential addition of

three RR constraints to a 4R serial chain [9]. This linkage graph and the input crank are used by an analysis algorithm developed by Parrish et al. [10].

The design of eight-bar linkages has been the focus of research by Mueller [12], who introduced a graphical approach for the synthesis of an eight-bar linkage. Also see the work of Hain [13] and Soni [14]. Angeles and Chen [15] developed a method to synthesize an eight-bar linkage obtained by coupling two four-bar linkages that can reach 11 task positions. Soh and McCarthy [2] obtained eight-bar linkages by adding two RR constraints to a 6R parallel robot. Sonawale and McCarthy [16] extended this procedure to a design system that not only synthesized the constrained 6R loops but analyzed the resulting eight-bar linkages to verify performance.

The usefulness of eight-bar linkages is demonstrated by Kempe [17], who shows that the geometric properties of these linkages yield the Peaucellier straight-line linkage and Angle trisector. Similarly, Artobolevskii [18] shows that an eight-linkage can be sized to trace any quadratic curve.

The inspiration for our example is Dijksman's [19] demonstration that an eight-bar linkage that has a link with straight-line rectilinear motion is constructed from Hart's straight-line six-bar linkage. Our design procedure does not rely on the special geometric relationships that are central to the design of these eight-bar linkages, and obtains over 800 eight-bar linkages that guide an end-effector though five task positions along straight-line rectilinear movement.

3 The Design Procedure

In order to design an eight-bar linkage, we begin with a 4R serial chain and five required positions and orientations of its end-effector. With the end-effector positioned in each of the task positions, the inverse kinematics of the 4R chain determines the position and orientation of each of its links. The inverse kinematics equations have a free parameter that the designer can use to adjust the configuration of the chain. This provides control over the shape and movement of the resulting eight-bar linkage.

Once the position and orientation of every link in the 4R chain is determined in each of the five task positions, Burmester theory can be used to calculate RR constraints to connect pairs of links in the chain. The usual formulation of Burmester's synthesis equations assumes that the RR constraint is defined by identifying five positions of a moving body M_ν, $\nu = 1,\ldots,5$ relative to a fixed body F. In our application, an RR constraint connects two moving links that have five relative positions. Let R_ν, $\nu = 1,\ldots,5$ be a set of moving frame attached to one link and S_ν, $\nu = 1,\ldots,5$ be a set of frames attached to a second link in the 4R chain.

The positions and orientations of the frames R_ν and S_ν can be determined from the inverse kinematics of the 4R chain positioned in each of the required five task positions. Therefore, we have the five sets of 3×3 homogeneous transformations $[R_\nu]$ and $[S_\nu]$, $\nu = 1,\ldots,5$ measured relative to the ground frame G, given by,

$$[R_\nu] = \begin{bmatrix} \cos\theta_\nu & -\sin\theta_\nu & a_\nu \\ \sin\theta_\nu & \cos\theta_\nu & b_\nu \\ 0 & 0 & 1 \end{bmatrix}, \; [S_\nu] = \begin{bmatrix} \cos\phi_\nu & -\sin\phi_\nu & c_\nu \\ \sin\phi_\nu & \cos\phi_\nu & d_\nu \\ 0 & 0 & 1 \end{bmatrix}, \quad \nu = 1,\ldots,5. \quad (1)$$

Introduce the coordinates $\mathbf{W}^\nu$ of a joint attached in frames R_ν for one link, and $\mathbf{G}^\nu$ of a joint attached in frames S_ν for a second link, all measured in the ground frame G. Then the condition that these joints form an RR crank is given by

$$(\mathbf{W}^\nu - \mathbf{G}^\nu)\cdot(\mathbf{W}^\nu - \mathbf{G}^\nu) = R^2, \; \nu = 1,\ldots,5, \quad (2)$$

where the dot denotes the usual vector dot product, and R is a constant that defines the length of the RR crank.

It is convenient to introduce the relative transformations

$$[R_{1\nu}] = [R_\nu][R_1]^{-1} \quad [S_{1\nu}] = [S_\nu][S_1]^{-1}, \quad \nu = 1,\ldots,5, \quad (3)$$

so that $\mathbf{W}^1 = (x, y, 1)$ and $\mathbf{G}^1 = (u, v, 1)$ are independent variables, and

$$\mathbf{G}^\nu = [R_{1\nu}]\mathbf{G}^1 \quad \mathbf{W}^\nu = [S_{1\nu}]\mathbf{W}^1, \quad \nu = 1,\ldots,5. \quad (4)$$

The constraint equations for the RR crank now take the form,

$$([S_{1\nu}]\mathbf{W}^1 - [R_{1\nu}]\mathbf{G}^1)\cdot([S_{1\nu}]\mathbf{W}^1 - [R_{1\nu}]\mathbf{G}^1) = R^2 \quad \nu = 1,\ldots,5. \quad (5)$$

Subtract the first of the equations (5) from the remaining to eliminate R^2 and obtain the four bilinear synthesis equations in four unknowns $\{u, v, x, y\}$ as,

$$([S_{1\nu}]\mathbf{W}^1 - [R_{1\nu}]\mathbf{G}^1)\cdot([S_{1\nu}]\mathbf{W}^1 - [R_{1\nu}]\mathbf{G}^1) - (\mathbf{W}^1 - \mathbf{G}^1)\cdot(\mathbf{W}^1 - \mathbf{G}^1) = 0, \quad \nu = 2,\ldots,5. \quad (6)$$

The roots of these synthesis equations yields as many as four sets of design parameters, $\mathbf{r}_= (u_i, v_i, x_i, y_i)$, $i = 1,2,3,4$, defining the RR cranks $\mathbf{G}^1\mathbf{W}^1$ [3,5,8].

Once the RR constraints are computed they are assembled into eight-bar linkages to yield candidate designs. The many ways that these RR cranks can be attached to the 4R chain is presented in detail in what follows, and listed in the Appendix.

Each design obtained in this process is analyzed to determine that its end-effector passes through the required task positions in a single assembly of the eight-bar linkage. McCarthy and Choe [20] show that kinematic synthesis equations regularly fail to yield designs that meet this basic feasibility requirement. This challenge is overcome by introducing small variations to the task within designer specified tolerance zones [21].

The design algorithm starts by designing eight-bar linkages for the required task positions, $(\phi_\nu, \mathbf{d}_\nu)$, $\nu = 1,\ldots,5$. Then the algorithm is iterated q additional times with these task positions modified by a random selection, $(\pm\Delta\phi_\nu, \pm\Delta\mathbf{d}_\nu)$, $\nu = 1,\ldots,5$, within user defined tolerance zones,

$$\{(\phi_\nu, \mathbf{d}_\nu), \nu = 1,\ldots,5\}_k = \{(\phi_i, \mathbf{d}_\nu), \nu = 1,\ldots,5\} + \{\text{Rand}(\pm\Delta\phi_\nu, \pm\Delta\mathbf{d}_\nu), \nu = 1,\ldots,5\}, \quad k = 1,\ldots,q. \tag{7}$$

In each iteration the feasible designs are saved and the result is an effective design system for eight-bar linkages.

4 Attachment of RR Constraints to a 4R Serial Chain

In this section, we present a systematic process that identifies attachment locations for a set of three RR constraints that transform a 4R serial chain into an eight-bar linkage. To do this we introduce the linkage graph [9] for a 4R chain given by $G =< V, E >$, where the list of links V form the vertices of the graph and the list of edges E represents the joints in the linkage. Thus, the linkage graph G of a 4R chain is given by

$$G =< V, E > = < \{1,2,3,4,5\}, \{\{1,2\},\{2,3\},\{3,4\},\{4,5\}\} > \tag{8}$$

Note that link 1 is the ground and link 5 is the end-effector. See Figure 1.

Our goal is to enumerate the linkage graphs L that are obtained from G by adding three subgraphs, each adding a vertex and two edges that represent an RR crank, in a way that reduces the four degrees of freedom of the 4R chain to one degree-of-freedom.

Denote the three RR constraints as the subgraphs,

$$\begin{aligned} A_{ij} &= < \{i,j,6\}, \{\{i,6\},\{j,6\}\} >, \\ B_{kl} &= < \{k,l,7\}, \{\{k,7\},\{l,7\}\} >, \\ C_{mn} &= < \{m,n,8\}, \{\{m,8\},\{n,8\}\} >, \end{aligned} \tag{9}$$

where the vertices (i,j), (k,l) and (m,n) are to be enumerated to determine all possible eight-bar linkages. The linkage graph, $L_{(ij)(kl)(mn)}$, obtained by the addition of these RR constraints is given by,

$$L_{(ij)(kl)(mn)} = G \cup \{\{6,7,8\}, \{\{i,6\},\{j,6\},\{k,7\},\{l,7\},\{m,8\},\{n,8\}\}\}, \tag{10}$$

In order to enumerate the linkage graphs, $L_{(ij)(kl)(mn)}$, we introduce the notation V_5 for the vertex list of the 4R chain, V_6 for the vertex list of the linkage after A_{ij} is attached, and similarly let V_7 be the vertex list after both A_{ij} and B_{kl} are attached. The lists P_A, P_B and P_C formed from pairs of vertices in the lists V_5, V_6 and V_7 that are available for the attachment of the RR constraints A_{ij}, B_{kl} and C_{mn} are given by

$$\begin{aligned} P_A &= \{(i,j) : i,j \in V_5, i \neq j\}, |P_A| = \binom{5}{2} = 10, \\ P_B &= \{(k,l) : k,l \in V_6, k \neq l\}, |P_B| = \binom{6}{2} = 15 \\ P_C &= \{(m,n) : m,n \in V_7, m \neq n\}, |P_C| = \binom{7}{2} = 21. \end{aligned} \tag{11}$$

Thus, the maximum number of linkage graphs, $L_{(ij)(kl)(mn)}$, that can be obtained from the attachment of three RR chains to a 4R chain is given by,

$$|L_{(ij)(kl)(mn)}| = |P_A||P_B||P_C| = 3150. \tag{12}$$

This enumeration process yields 3150 sets of three RR attachments that we denote as $(ij)(kl)(mn)$.

Ordering: In order to eliminate duplicates from the list of linkage graphs, introduce the convention,

$$i < j, \quad k < l, \quad m < n. \tag{13}$$

Notice that the three RR constraints, $(ij)(kl)(mn)$, have vertex 6 only in (kl) or (mn) and vertex 7 only in (mn). This leads to an ordering for the linkage graphs given by:

1. if $(ij)(kl)(mn)$ do not include vertices 6 and 7, then order by the first entry followed by the second entry;
2. if $(ij)(kl)(mn)$ includes the vertex 6, insert it as (mn) and sort $(ij)(kl)$ by the first entry followed by the second entry,
3. if $(ij)(kl)(mn)$ includes the vertex 6 twice, insert it as $(kl)(mn)$ and sort by the first entry followed by the second entry.

This ordering makes it possible to identify and eliminate duplicate sets of three RR constraints, which reduces the number of linkage graphs from 3150 to 1275.

Structure Subgraphs: This list of 1275 linkage graphs reduces further by eliminating the graphs that have the following features:

1. Three edges form a triangle, $\{\{i,j\},\{j,k\},\{k,i\}\}$. If three links are connected by three joints, it forms a structure with no relative movement. A typical example is shown in Figure 2;
2. A vertex is connected across vertex pairs (i,k) or (j,l) that are opposite sides of a four-bar sub-chain, $\{\{i,j\},\{j,k\},\{k,l\},\{l,i\}\}$. In this case, the five vertices forms a structure with no relative movement. Typical examples include the ones shown in Figure 3 and 4; and

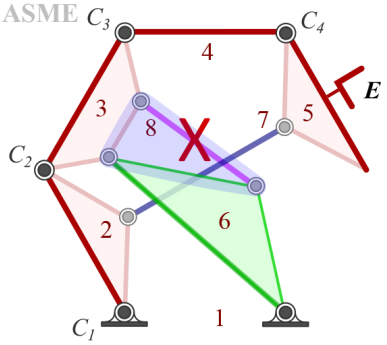

(13)(25)(36)

Fig. 2. The RR constraints A_{13} and C_{36} connect the links $\{3,6,8\}$ to form a triangular structure, thus the linkage graph $L_{(13)(25)(36)}$ is invalid.

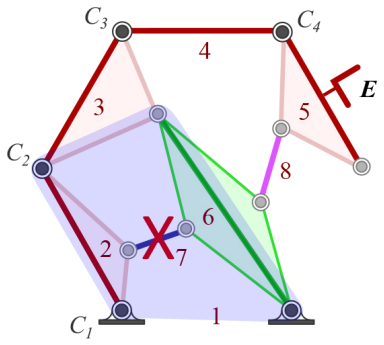

(13)(26)(56)

Fig. 3. The RR constraint A_{13} forms a quadrilateral loop with links $\{1,2,3,6\}$. The RR constraint B_{26} transforms this loop into a structure, so linkage graph $L_{(13)(26)(56)}$ is invalid.

3. Link 1 and link 5 should be connected to the rest of the links by at least 2 edges. A couple of typical examples of invalid linkage graphs that do not satisfy this are shown in Figure 5.

The reduces the number of linkage graphs to 152.

Design features: Finally, we impose the constraint that only two edges are connected to the base frame. This reduces the demand on the designer to accommodate bearing ground supports for the linkage. The result of these conditions reduces the number of linkage graphs to 100 unique eight-bar linkage graphs.

Task configurations: Given the linkage graph $L_{(ij)(kl)(mn)}$ for an eight-bar linkage, the position and orientation of each link $\mu = 1,\ldots,8$ is defined by the transformation,

$$[K_{\mu,\nu}] = \begin{bmatrix} \cos\theta_{\mu,\nu} & -\sin\theta_{\mu,\nu} & a_{\mu,\nu} \\ \sin\theta_{\mu,\nu} & \cos\theta_{\mu,\nu} & b_{\mu,\nu} \\ 0 & 0 & 1 \end{bmatrix}, \ \mu = 1,\ldots,8, \ \nu = 1,\ldots,5, \tag{14}$$

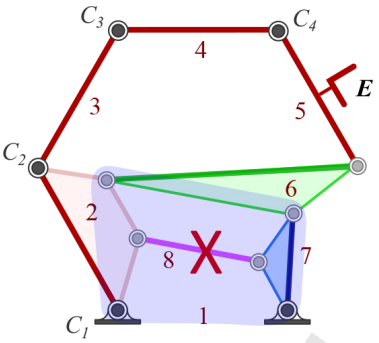

(25)(16)(27)

Fig. 4. The RR constraints A_{25} and B_{16} form the quadrilateral loop $\{1,2,6,7\}$, therefore, the RR constraint C_{27} causes this loop to become a structure. Thus, the linkage graph $L_{(25)(16)(27)}$ is invalid.

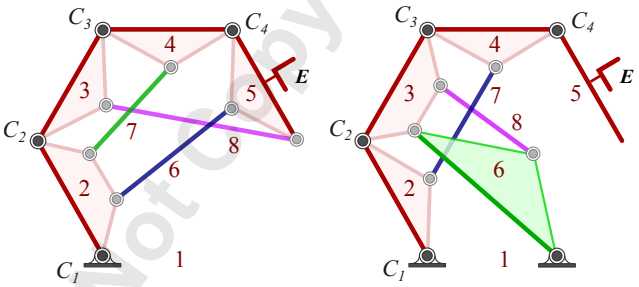

(a) (24)(25)(35) (b) (13)(24)(36)

Fig. 5. The linkage graphs $L_{(24)(25)(35)}$ and $L_{(13)(24)(36)}$ are invalid because all the links except one combine to form a structure. In (a) the structure rotates about the base pivot C_1, and in (b) the end-effector rotates around C_4 relative to the structure.

where $\nu = 1,\ldots,5$ denotes the five configurations of the 4R chain.

The RR constraint between the vertices $\{i,k\}$ obtained by solving the synthesis equations (6), with substitution,

$$[R_\nu] = [K_{i,\nu}], \ [S_\nu] = [K_{k,\nu}], \quad \nu = 1,\ldots,5, \tag{15}$$

where ν indexes the five positions of the link frames R_ν and S_ν.

5 Specifying the Design Requirements

The design requirements for the eight-bar linkage are provided by five configurations of a 4R serial chain. This is achieved by specifying:

1. the coordinates $\mathbf{g} = (g_x, g_y, 1)$ of the base joint C_1 in the ground frame G;
2. the dimensions, l_2, l_3, l_4, of the four links in the serial chain, see Figure 6;
3. the vector $\mathbf{h} = (h_x, h_y, 1)$ from the last joint C_4 to the end-effector frame in the end-effector frame H;

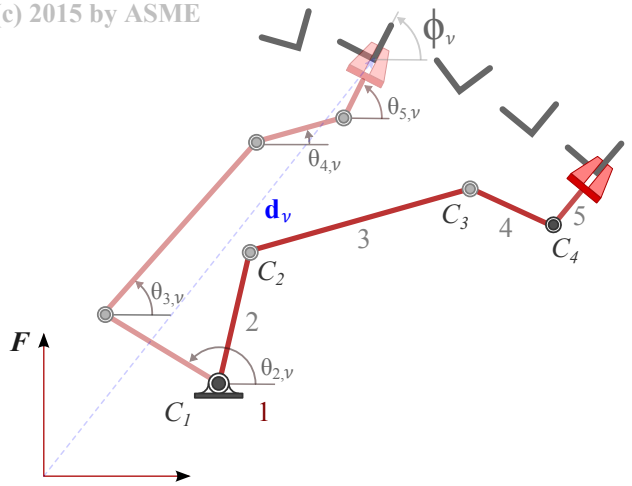

Fig. 6. The user-defined 4R chain is shown in the first and fourth position. In this case, the end-joint C_4 is positioned on the x-axis of the end-effector frame.

4. the origin of the task frames $\mathbf{d}_\nu = (a_\nu, b_\nu)$ and their orientation ϕ_ν, shown in Figure 6, yield the five transformations

$$D_\nu = \begin{bmatrix} \cos\phi_\nu & -\sin\phi_\nu & a_\nu \\ \sin\phi_\nu & \cos\phi_\nu & b_\nu \\ 0 & 0 & 1 \end{bmatrix}, \nu = 1, \ldots, 5; \qquad (16)$$

and,

5. when the end-effector positioned in each task position, the 4R chain becomes a four-bar linkage that has a degree-of-freedom that the designer is free to specify, Figure 7.

6 Kinematics of the 4R Chain

The kinematics equations of the 4R chain are given by the vector loop equations measured from the origin of the fixed frame F to the origin of the end-effector frame H. Introduce the three link vectors $\mathbf{a}_2 = C_1C_2$, $\mathbf{a}_3 = C_2C_3$, and $\mathbf{a}_4 = C_3C_4$, and compute their coordinates $\mathbf{a}_\mu = (x_\mu, y_\mu)$ in each task position ν,

$$\begin{Bmatrix} x_{\mu,\nu} \\ y_{\mu,\nu} \end{Bmatrix} = \begin{bmatrix} \cos\theta_{\mu,\nu} & \sin\theta_{\mu,\nu} \\ \sin\theta_{\mu,\nu} & \cos\theta_{\mu,\nu} \end{bmatrix} \begin{Bmatrix} l_\mu \\ 0 \end{Bmatrix}, \qquad (17)$$

or

$$\mathbf{a}_{\mu,\nu} = [R(\theta_{\mu,\nu})]\mathbf{l}_\mu, \quad \mu = 2,3,4, \ \nu = 1, \ldots 5. \qquad (18)$$

The kinematics equations of the 4R chain take the form

$$\mathbf{d}_\nu = \mathbf{g} + \mathbf{a}_{2,\nu} + \mathbf{a}_{3,\nu} + \mathbf{a}_{4,\nu} + [R(\phi_\nu)]\mathbf{h}, \ \nu = 1, \ldots, 5. \qquad (19)$$

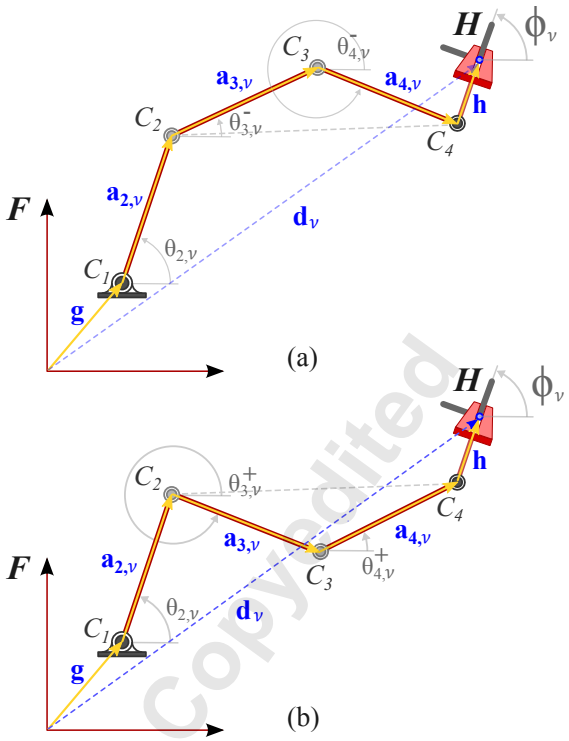

Fig. 7. When the end-effector of the 4R chain is in each task positions the remaining bars form a quadrilateral loop with the free parameter θ_2. For each value of θ_2 there are two configurations of the 4R chain, (a) elbow up and (b) elbow down.

When the end-effector is positioned in the task frame, the 4R chain forms a four-bar linkage, defined by the quadrilateral $C_1C_2C_3C_4$. This means the angles $\theta_{2,\nu}$ are free parameters that are specified by the designer. The remaining angles $\theta_{3,\nu}$ and $\theta_{4,\nu}$ then defined by the condition,

$$|(\mathbf{g} + \mathbf{a}_{2,\nu}) - (\mathbf{d}_\nu - [R(\phi_\nu)]\mathbf{h} - \mathbf{a}_{4,\nu})| = l_3^2 \qquad (20)$$

This equation can be solved to determine $\theta_{4,\nu}$ using the analysis of a four-bar linkage, at which point $\theta_{3,\nu}$ can also be determined. See McCarthy and Soh [8].

For a given value of the joint angle $\theta_{2,\nu}$, the four-bar linkage has two configurations $\theta^+_{4,\nu}$ such that C_3 is below the diagonal C_2C_4 called the elbow down configuration, or $\theta^-_{4,\nu}$ with C_3 above this diagonal or elbow up, Figure 7. The selection of the joint angle $\theta_{2,\nu}$ and the configuration of the 4R chain defines the position of each link for the 4R chain in each of the task positions. This defines the transformations $[K_{\mu,\nu}]$, $\mu = 2,3,4,5$ and $\nu = 1, \ldots, 5$.

In the formulation of the specifications for the synthesis of an eight-bar linkage it is convenient to select equal values for the link lengths of the 4R chain, that is

$$l = l_2 = l_3 = l_4, \qquad (21)$$

then equation (20) is used to determine the configuration of the 4R chain for given values of $\theta_{2,j}$. In this case, the sym-

metry of the four-bar linkage can cause problems with the synthesis equations, therefore asymmetry between $\theta_{2,j}$ and $\theta_{4,j}$ is required to ensure a complete solution of the synthesis equations.

7 Calculating Candidate Designs

The design system solves the synthesis equations (6), to calculate the three RR constraints, for each of the 100 unique linkage graphs, $L_{(ij)(kl)(mn)}$. The number of solutions must account for RR constraint solutions that satisfy the synthesis equations and are already part of the linkage.

This is done by distinguishing three cases, (i) sets of three RR constraints that include only the vertices, $\{1,2,3,4,5\}$, of the original 4R chain, (ii) sets of three RR constraints that include one connection to a vertex in the set $\{6,7\}$, and (iii) sets of three RR constraints that include connections to vertices $\{6,7\}$.

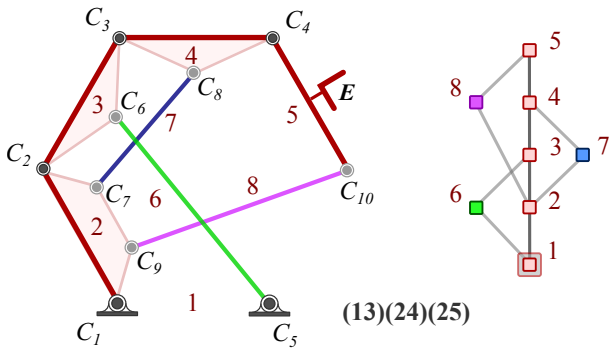

Fig. 8. An eight-bar linkage with the graph $L_{(13)(24)(25)}$ that has three independent RR constraints.

Independent constraints: A set of three RR constraints that connect to the vertices $i,j,k,l,m,n \in \{1,2,3,4,5\}$ can be applied independently. In order to count the number of design candidates obtained from the synthesis equations, consider the linkage graph $(13)(24)(35)$ shown in Figure 8. Of the $\binom{5}{3} = 20$ ways to select these attachments 12 are unique and are shown in Figure 14 in the Appendix.

Observe that for the attachment of the first RR constraint A_{13}, one solution C_1C_2 already exists, thus the synthesis equations yield at most three new RR constraints. This is true for the second RR constraint B_{24} as well. In contrast, the third RR constraint C_{27} does not bridge an existing constraint so all four RR solutions are available. In this case, the combinations of the RR solutions yields as many as $3 \times 3 \times 4 = 36$ candidate designs.

The synthesis equations for the 12 linkage graphs with independent constraints yields as many as 429 eight-bar linkage candidate designs.

Level one constraints: A set of three RR constraints with $i,j,k,l \in \{1,2,3,4,5\}$, $m \in \{1,2,3,4,5,6\}$ and $n \in \{6,7\}$,

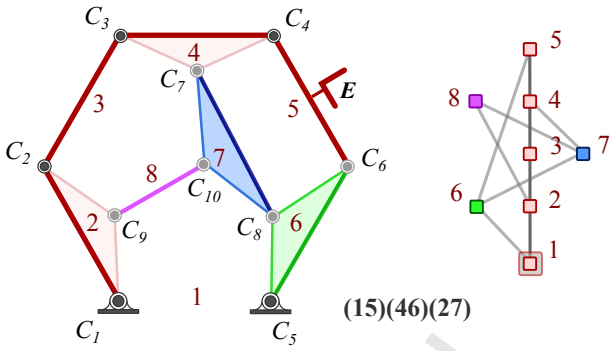

Fig. 9. An eight-bar linkage with the graph $L_{(15)(46)(27)}$ with the second-level dependent RR constraint, C_{27}.

is said to have first level dependence because it includes a connection to a previously designed RR constraint. There are 48 first level dependent linkage graphs as shown in Figure 15, 16 and 17 in the Appendix. The synthesis equations for these 48 first level dependent linkage graphs yield as many as 1895 candidate designs.

Level two constraints: A set of three RR ,constraints with $i,j,k,m \in \{1,2,3,4,5\}$, $l \in \{6\}$ and $n \in \{6,7\}$, is said to have second level dependent because it includes connections to both previously designed RR constraints. There are 40 second level dependent linkage graphs as shown in Figure 18 and 19 in the Appendix.

The number of solutions to the synthesis equations for second level constraints is shown in Figure 9. The synthesis equations for the RR constraint A_{15} has as many as four solutions, while the second RR constraint B_{46} has three, since the C_4C_6 already exists. The third RR constraint C_{27} has all the four RR solutions. Thus, there are as many as $4 \times 3 \times 4 = 48$ candidate designs for this case. The synthesis equations for the 40 second level dependent linkage graphs yield as many as 1627 candidate designs.

Total count: This design procedure yields as many as 3951 eight-bar linkage candidate designs for the 100 linkage graphs.

8 Identifying Feasible Designs

Each eight-bar linkage obtained from the synthesis equations is analyzed to determine the feasibility of its movement through the task positions in every assembly. In order to be a feasible design, the end-effector must pass through the five task positions while the eight-bar linkage is in a single assembly.

We use the automated system developed by Parrish et al. [10] for the analysis of eight-bar linkages. This algorithm reads the location of the pivots of the eight-bar linkage in the first task position and the incidence matrix of the linkage graph to formulate the three loop equations of the eight-bar linkage. These equations are solved analytically using the

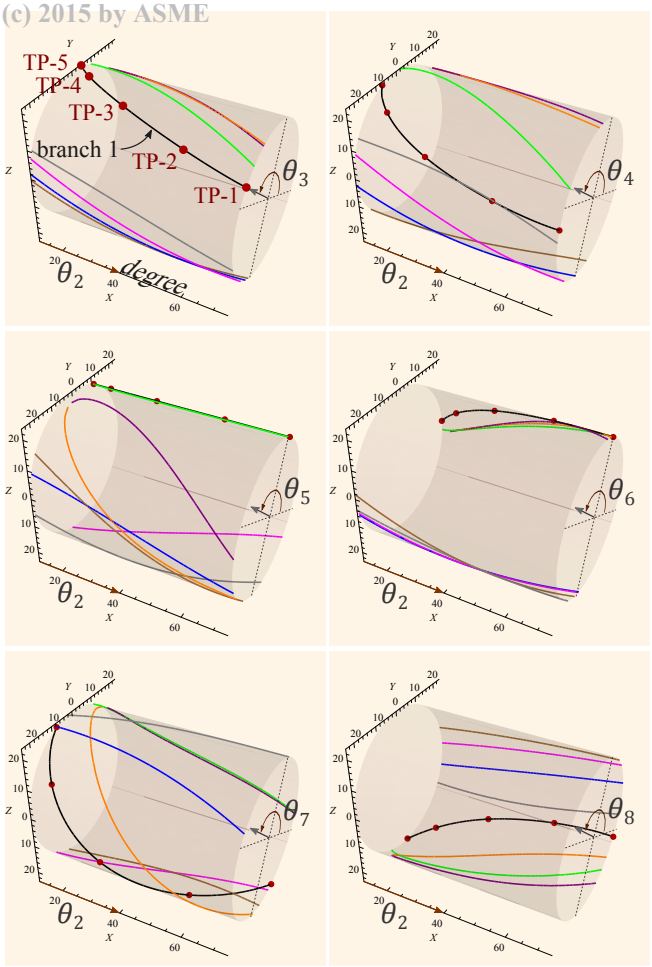

Fig. 10. Analysis of each eight-bar linkage determines if the five task positions lie on a single linkage assembly. Only linkages that satisfy this condition are feasible.

Dixon determinant approach in order to obtain all the assemblies of the linkage at each value of the input angle.

A sorting algorithm collects the result of the analysis routine into a maximum of 16 assemblies that define the values of the 10 joint angles for k iterations of the input angle θ_2. Note that θ_1 is the angle made by the ground link which remains constant. The results are the joint trajectories for each of the 16 assemblies,

$$\begin{aligned}\Theta_1 &= \{\{\theta_{1,1}, \theta_{1,2}, \ldots, \theta_{1,10}\}_k\}, \quad k = 1, \ldots, n,\\ \Theta_2 &= \{\{\theta_{2,1}, \theta_{2,2}, \ldots, \theta_{2,10}\}_k\}, \quad k = 1, \ldots, n,\\ &\vdots\\ \Theta_{16} &= \{\{\theta_{16,1}, \theta_{16,2}, \ldots, \theta_{16,10}\}_k\}, \quad k = 1, \ldots, n. \end{aligned} \tag{22}$$

For more details about sorting solutions into linkage assemblies to verify performance, see Plecnik and McCarthy [22].

Figure 10 is an example where each assembly trajectory is represented by its joint angle $\theta_3, \ldots, \theta_{10}$ trajectories, for the given input joint angle θ_2. In order to meet the performance requirements, all the task positions must lie on one trajectory, or branch, for all the joint angles. In addition to this requirement the designer may also require the link lengths of the linkage to meet certain criteria to be of practical use.

9 Five Rectilinear Positions on a Straight-line

In this section we seek eight-bar linkages that guide the end-effector in rectilinear movement along a straight-line, [19]. The five task positions selected are given in Table 1 and the user specified 4R chain information is given in Table 2. The tolerances for each task position $(\Delta\phi_j, \Delta\mathbf{d}_j), j = 1, \ldots, 5$ are given in Table 3. Notice that since the tolerances are specified on the task positions, the accuracy of rectilinear motion of the linkage solutions is limited to the tolerances specified.

Table 1. Five rectilinear task positions on a straight line.

Task	ϕ_v, $\mathbf{d}_v = (a_v, b_v)$
1	$0.0°$, $(0.0, 0.0)$
2	$0.0°$, $(22.0, 0.0)$
3	$0.0°$, $(50.0, 0.0)$
4	$0.0°$, $(78.0, 0.0)$
5	$0.0°$, $(100.0, 0.0)$

Table 2. The data defining the 4R chain.

Ground pivot C_1 in G,	$(50.0, -90.0, 0)$
End-effector pivot C_4 in H,	$(-3.54, -3.54)$
Link lengths, $l_2 = l_3 = l_4$,	45
Elbow position,	up.

Table 3. Tolerances on the five task positions.

Task	$\Delta\phi$, $\Delta\mathbf{d}$
1	$0.0°, (1.0, 0.001)$
2	$0.1°, (5.0, 0.001)$
3	$0.2°, (5.0, 0.001)$
4	$0.1°, (5.0, 0.001)$
5	$0.0°, (1.0, 0.001)$

An additional design criteria was imposed in order to eliminate very large and very small links. The distance

Table 4. The number of linkage candidates, feasible designs, and compute time for 1, 10 and 100 iterations.

Iterations	Candidates	Feasible designs	Compute time
1	1577	14	17.8 min
10	12179	108	141.94 min
100	110454	853	43 hr 52 min

Table 5. The joint coordinates for an example rectilinear eight-bar linkage obtained using the design procedure.

Pivot	Location Data (x,y)
C_1	$(50.0,-90.0,0)$
C_2	$(62.17,-46.68)$
C_3	$(41.35,-6.78)$
C_4	$(-3.54,-3.54)$
C_5	$(46.69,-39.86)$
C_6	$(56.43,-20.30)$
C_7	$(-4.65,15.47)$
C_8	$(4.75,11.67)$
C_9	$(104.60,-78.80)$
C_{10}	$(5.75,-15.33)$

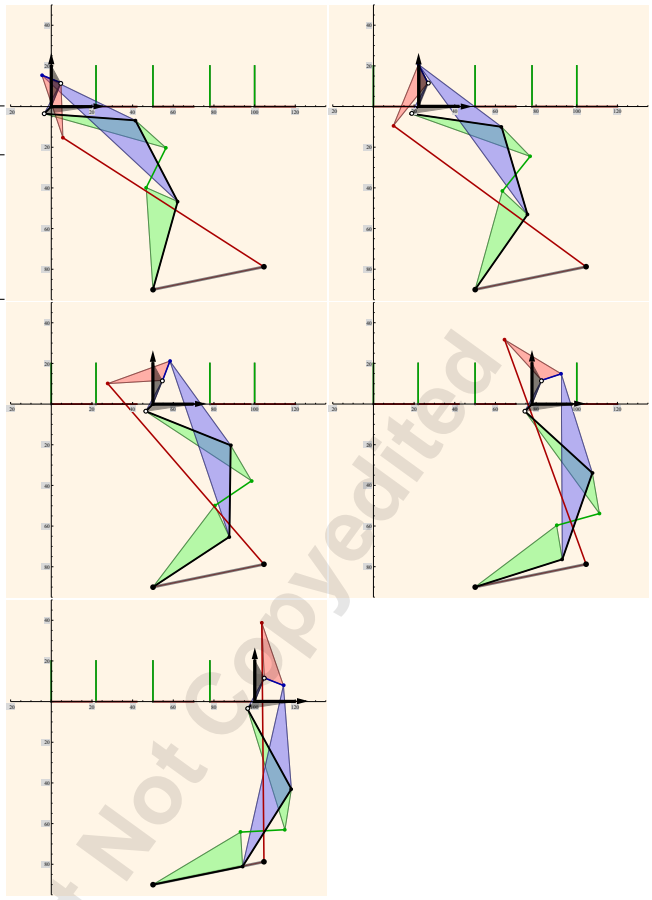

Fig. 11. Line drawing of the example rectilinear eight-bar linkage obtained from the design procedure.

$r = 200$ is selected by the designer and the allowable link lengths in eight-bar linkage candidates are limited to the range $0.01r \le l_\mu \le r$, $\mu = 1,\ldots,8$. The results for number of iterations $1, 10$ and100 are shown in Table 4. The calculations were performed on an AMD Phenom II, 3.3 GHz, 6 core Windows machine.

The joint coordinates of an example rectilinear eight-bar linkage with a deviation from specified task positions within the user defined tolerances are listed in Table 5. A line drawing of this rectilinear eight-bar linkage moving through the five task positions is shown in Figure 11. The three RR constraints are applied between the link pairs $(2,4)(3,5)(1,7)$ as shown in Figure 12. A solid model of the example rectilinear linkage is shown in Figure 13.

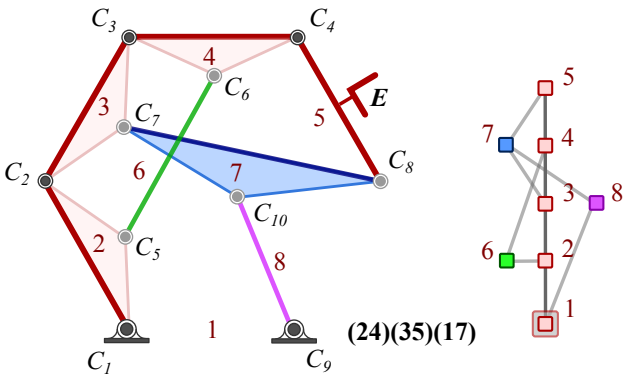

Fig. 12. The topology and linkage graph $L_{(24)(35)(17)}$ for the example rectilinear eight-bar linkage design.

10 Conclusions

This paper presents a new design procedure for eight-bar linkages that solves for as many as 3951 candidate designs obtained for 100 different linkage graphs by adding three RR constraints to a 4R serial chain. Existing design systems are limited to either special geometry or specific linkage graphs. This approach provides the designer flexibility to shape to movement of the linkage by defining five configurations of the 4R chain as well as the five task positions.

Each candidate design is analyzed to verify that the task positions lie on a single eight-bar linkage assembly. And, to increase the number of feasible eight-bar linkages the system introduces random variations within designer specified tolerance zones. The result is an effective eight-bar linkage design system.

An example set of five task positions along a straight line in rectilinear motion yielded 14 feasible eight-bar link-

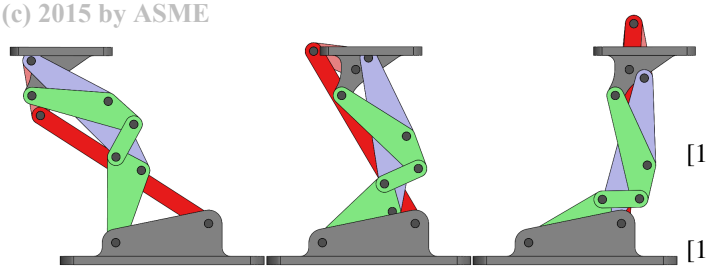

Fig. 13. A solid model of the rectilinear eight-bar linkage showing the rectilinear movement of the end-effector.

ages in 18 minutes, while 100 iterations yielded 853 feasible eight-bar linkages in almost two days of computation on a desktop computer. Thus, this design system can calculate a large number of eight-bar linkages that meet user-specified criteria.

11 Acknowledgements

This material is based upon work supported by the National Science Foundation under grants CMMI 1066082 and 1346738.

References

[1] Soh, G. S., Perez, A., and McCarthy, J. M., 2006, "The Kinematic Synthesis of Mechanically Constrained Planar 3R Chains," *Proceedings of the first European Conference on Mechanism Science* (EUCOMES), Obergurgl, Austria.

[2] Soh, G. S., and McCarthy, J. M., 2007, "Synthesis of Eight-Bar Linkages as Mechanically Constrained Parallel Robots," *12th IFToMM World Congress*, June 18-21, Besancon, France.

[3] Burmester, L., 1888, *Lehrbuch der Kinematik, Vol. 1, Die ebene Bewegung*, Leipzig.

[4] Koetsier, T., 1989, "The centenary of Ludwig Burmester's Lehrbuch der Kinematik," *Mechanism and Machine Theory*, 1:37-38.

[5] Sandor, G. N., and Erdman, A. G., 1984, *Advanced Mechanism Design: Analysis and Synthesis, Vol. 2*. Prentice-Hall, Englewood Cliffs, NJ.

[6] Burdick, J. W., 1989, "On the inverse kinematics of redundant manipulators: characterization of the self-motion manifolds," *1989 IEEE International Conference on Robotics and Automation*, 1:264-270, May 14-19, Scottsdale, AZ.

[7] Murray, R. M., Li, Z., and Sastry, S. S., 1994, *A Mathematical Introduction to Robotics Manipulators*, CRC Press, 456 pp.

[8] McCarthy, J. M. and Soh, G. S., 2010, *Geometric Design of Linkages. 2nd Ed.*, Springer-Verlag.

[9] Tsai L. W., 2000, *Mechanism Design: Enumeration of Kinematic Structures According to Function*, CRC Press.

[10] Parrish, B. E., McCarthy, J. M., and Eppstein, D., 2015,"Automated Generation of Linkage Loop Equations for Planar 1-DoF Linkages Demonstrated up to 8-bar," *ASME Journal of Mechanisms and Robotics*, February, Vol. 7.

[11] Parrish, B. E., 2014, "Automated Configuration Analysis of Planar Eight-Bar Linkages", PhD. dissertation, University of California, Irvine, CA, USA.

[12] Mueller, J., 1954, "Design Procedures for the Determination of Dimensions of Eight-bar and Ten-bar Linkages," PhD. dissertation, Technische Universitat Dresden, Germany.

[13] Hain, K., 1967, "The Simultaneous Production of Two Rectilinear Translations by Means of Eight-link Mechanisms.", *Journal of Mechanisms*, Vol. 2, No. 2, pp. 185-191.

[14] Hamid, S., and Soni A. H., 1973, "Synthesis of an Eight-Link Mechanism for Varieties of Motion Programs." *Journal of Engineering for Industry*, 95, no. 3, pp. 744-750.

[15] Chen, C., and Angeles, J., 2008, "A novel family of linkages for advanced motion synthesis.", *Mechanism and Machine Theory*, 43(7), pp. 882-890.

[16] Sonawale, K. H., and McCarthy, J. M., 2014, "Synthesis of Useful Eight-bar Linkages as Constrained 6R loops.", *Proceedings of the ASME 2014 International Design Engineering Technical Conferences and Computers and Information in Engineering Conference*, DET2014-35523, August 17-20, Buffalo, New York, USA.

[17] Kempe, A. B., 1877, *How To Draw a Straight Line: A lecture on linkages*, MacMillan and Co., 47pp.

[18] Artobolevskii, I. I., 1964, *Mechanisms for the Generation of Plane Curves*, (Trans. R. D. Wills), Pergamon Press, Oxford.

[19] Dijksman, E. A., 1994, "True Straight-line Linkages Having a Rectilinear Translating Bar," *Advances in Robot Kinematics and Computational Geometry* (eds. A. J. Lenarcic and B. B. Ravani), Kluwer Academic Publishers, pp 411-420.

[20] McCarthy, J. M., and Choe, J., 2010, "Difficulty of Kinematic Synthesis of Usable Constrained Planar 6R Robots," *Advances in Robot Kinematics*, 12th International Symposium, June 28 July 1, Portoroz, Slovenia.

[21] Sonawale, K. H., Arredondo, A., and McCarthy, J. M., 2013, "Computer Aided Design of Useful Spherical Watt I Six-bar Linkages," *Proceedings of the ASME 2013 International Design Engineering Technical Conferences and Computers and Information in Engineering Conference*, DET2013-13454, August 4-7, Portland, Oregon USA.

[22] Plecnik, M. M. and McCarthy, J. M., 2013, "Numerical Synthesis of Six-bar Linkages for Mechanical Computation," *Journal of Mechanisms and Robotics*, 031012, Vol. 6, August.

Journal of Mechanisms and Robotics. Received March 09, 2015;
Accepted manuscript posted July 10, 2015. doi:10.1115/1.4031026

Appendix: Eight-bar linkage graphs obtained by attaching three RR constraint to a 4R serial chain

The following figures present the 100 eight-bar linkage schematics and associated linkage graphs $L_{(ij)(kl)(mn)}$ that are obtained by the application of three RR constraints. They are separated into (i) 12 eight-bar linkages with independent constraints, which are those that have $i,j,k,l,m,n \in \{1,2,3,4,5\}$, Figure 14, (ii) 48 eight-bar linkages with level one constraints, which are those that have $i,j,k,l \in \{1,2,3,4,5\}$, $m \in \{1,2,3,4,5,6\}$ and $n \in \{6,7\}$, Figure 15, 16 and 17, and (iii) 40 eight-bar linkages with level two constraints, which are those with $i,j,k,m \in \{1,2,3,4,5\}$, $l \in \{6\}$ and $n \in \{6,7\}$, Figure 18 and 19 .

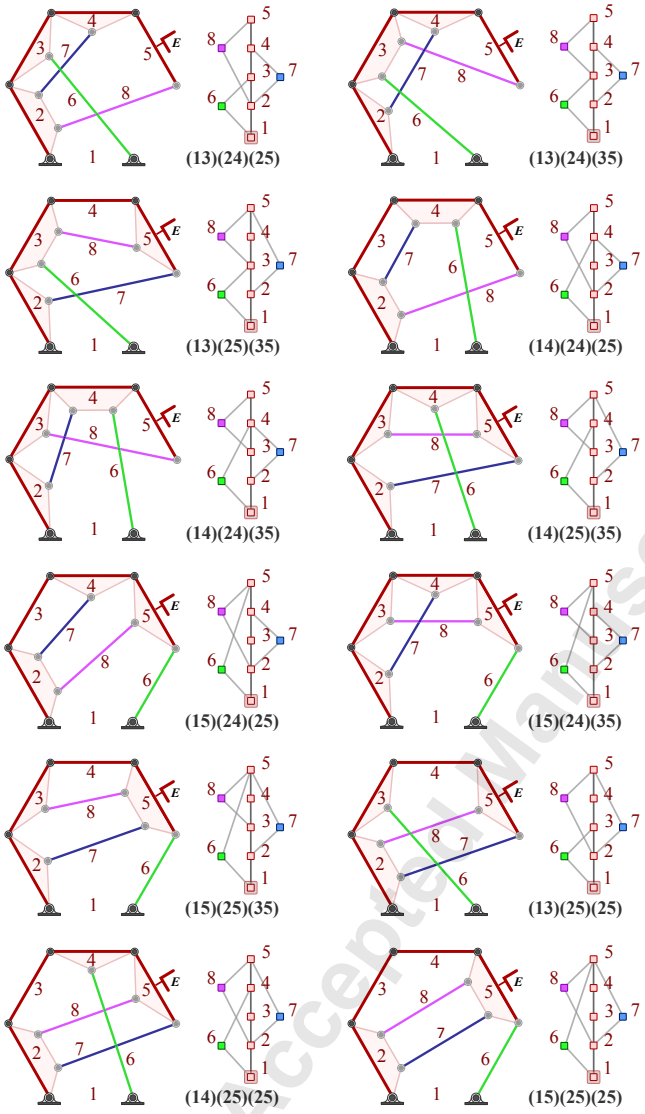

Fig. 14. The 12 eight-bar linkages obtained from three independent RR constraints, with $i,j,k,l,m,n \in \{1,2,3,4,5\}$.

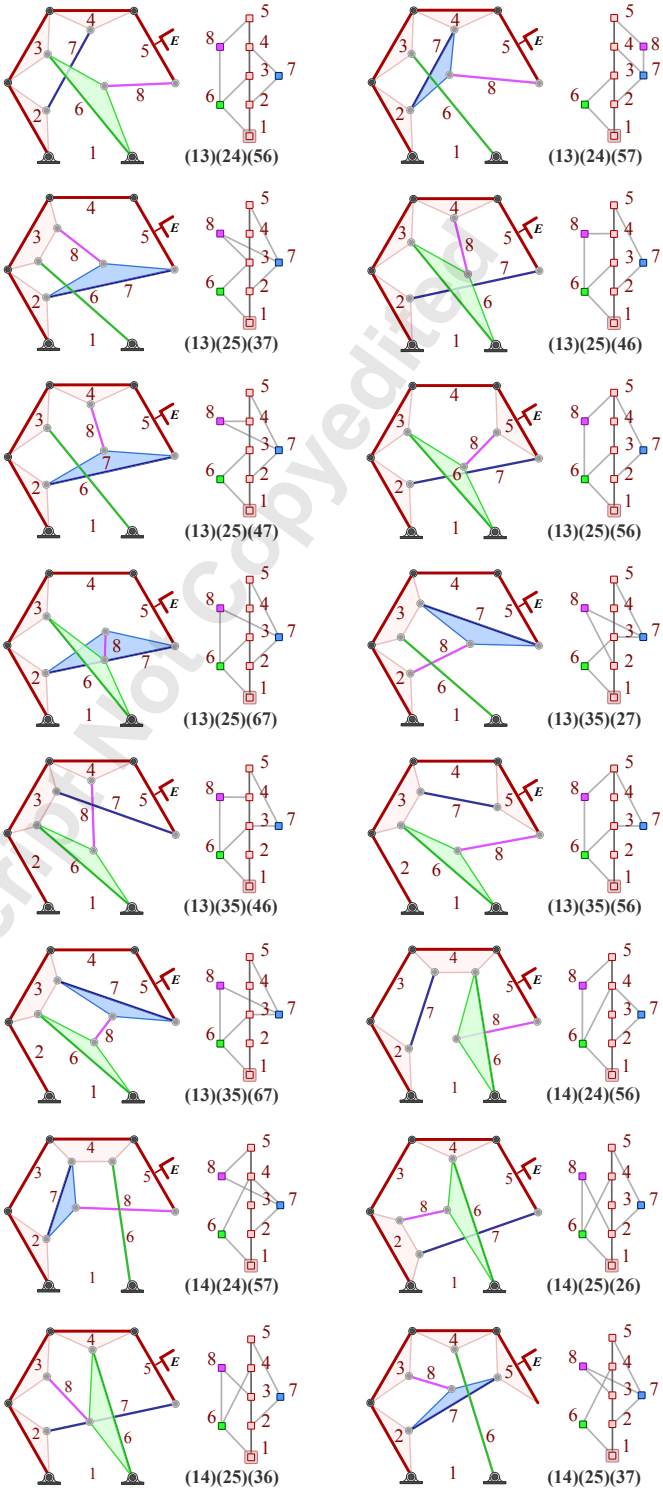

Fig. 15. Eight-bar linkages 1–16 of 48 with level one constraints, which are those with $i,j,k,l \in \{1,2,3,4,5\}$, $m \in \{1,2,3,4,5,6\}$ and $n \in \{6,7\}$.

Journal of Mechanisms and Robotics. Received March 09, 2015;
Accepted manuscript posted July 10, 2015. doi:10.1115/1.4031026

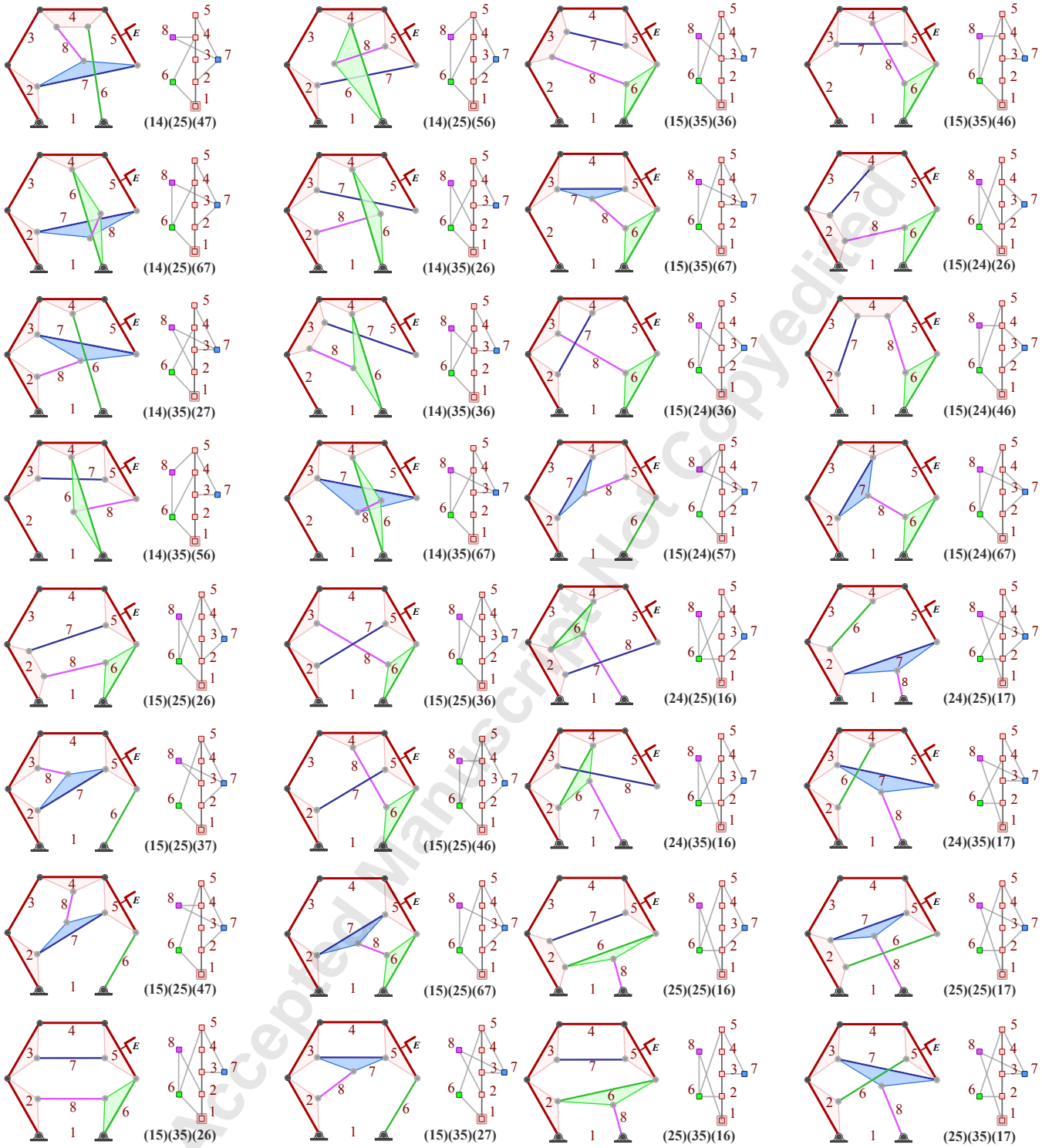

Fig. 16. Eight-bar linkages 17–32 of 48 with level one constraints, which are those with $i, j, k, l \in \{1,2,3,4,5\}, m \in \{1,2,3,4,5,6\}$ and $n \in \{6,7\}$.

Fig. 17. Eight-bar linkages 33-48 of 48 with level one constraints, which are those with $i, j, k, l \in \{1,2,3,4,5\}, m \in \{1,2,3,4,5,6\}$ and $n \in \{6,7\}$.

Journal of Mechanisms and Robotics. Received March 09, 2015;
Accepted manuscript posted July 10, 2015. doi:10.1115/1.4031026

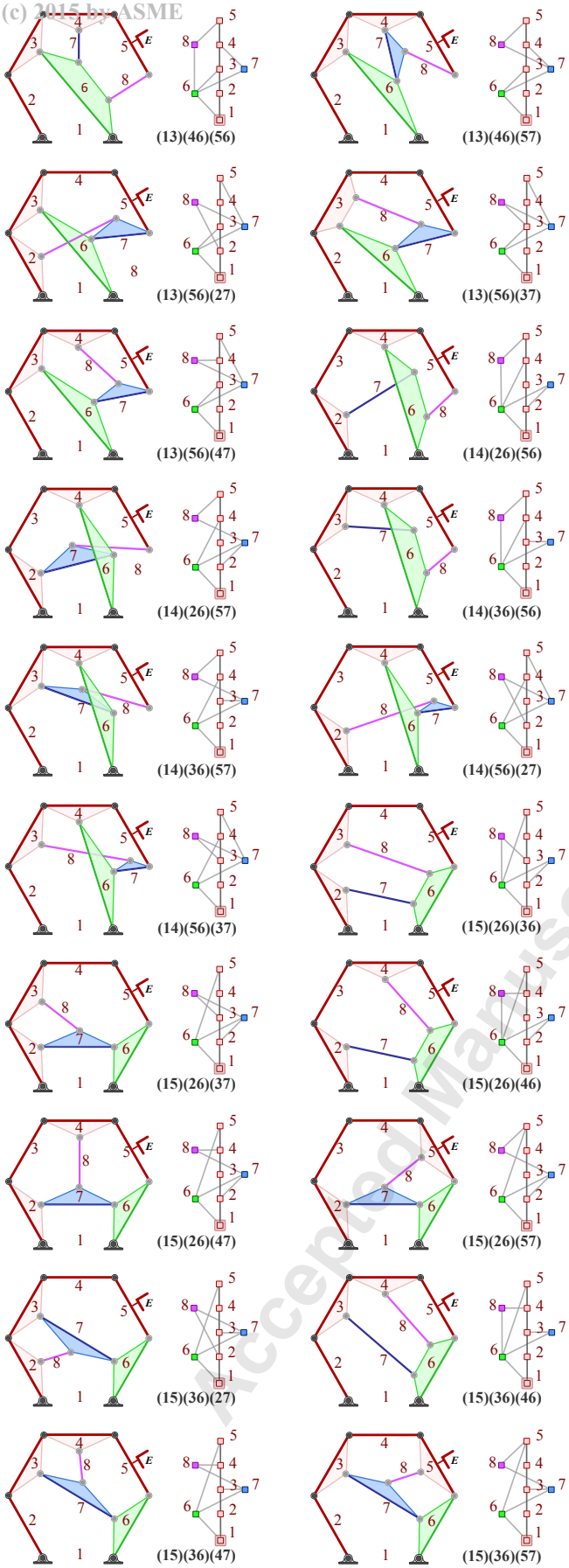

Fig. 18. Eight-bar linkages 1–20 of 40 with level two constraints, which are those with $i, j, k, m \in \{1,2,3,4,5\}, l \in \{6\}, n \in \{6,7\}$.

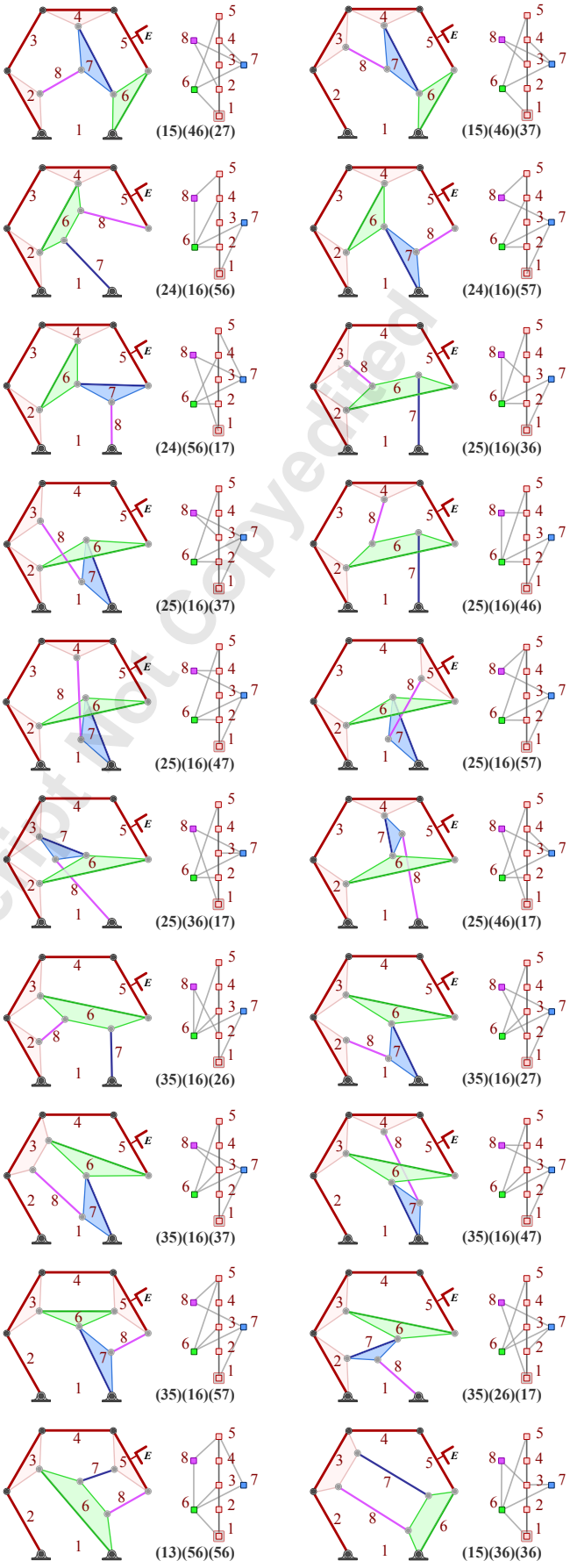

Fig. 19. Eight-bar linkages 21–40 of 40 with level two constraints, which are those with $i, j, k, m \in \{1,2,3,4,5\}, l \in \{6\}, n \in \{6,7\}$.

List of Figures

List of Tables